the plant journal

SEB Society for Experimental Biology

The Plant Journal (2014) **79,** 413–426 doi: 10.1111/tpj.12567

Post-transcriptional control of *GRF* transcription factors by microRNA miR396 and GIF co-activator affects leaf size and longevity

Juan M. Debernardi[1], Martin A. Mecchia[1], Liesbeth Vercruyssen[2], Cezary Smaczniak[3], Kerstin Kaufmann[3,†], Dirk Inze[2], Ramiro E. Rodriguez[1] and Javier F. Palatnik[1,*]

[1]*Instituto de Biología Molecular y Celular de Rosario (IBR), CONICET, Facultad de Ciencias Bioquímicas y Farmacéuticas, Universidad Nacional de Rosario, Ocampo y Esmeralda, Rosario, Argentina,*

[2]*Department of Plant Systems Biology, VIB, 9052 Ghent, Belgium, and*

[3]*Laboratory of Molecular Biology, Wageningen University, 6708PB Wageningen, The Netherlands*

Received 7 January 2014; revised 8 May 2014; accepted 21 May 2014; published online 2 June 2014.

*For correspondence (e-mail palatnik@ibr-conicet.gov.ar).

[†]Present address: Institute for Biochemistry and Biology, Potsdam University, 14476 Potsdam-Golm, Germany.

SUMMARY

The growth-regulating factors (GRFs) are plant-specific transcription factors. They form complexes with GRF-interacting factors (GIFs), a small family of transcriptional co-activators. In *Arabidopsis thaliana,* seven out of the nine *GRFs* are controlled by microRNA miR396. Analysis of Arabidopsis plants carrying a *GRF3* allele insensitive to miR396 revealed a strong boost in the number of cells in leaves, which was further enhanced synergistically by an additional increase of *GIF1* levels. Genetic experiments revealed that *GRF3* can still increase cell number in *gif1* mutants, albeit to a much lesser extent. Genome-wide transcript profiling indicated that the simultaneous increase of *GRF3* and *GIF1* levels causes additional effects in gene expression compared to either of the transgenes alone. We observed that GIF1 interacts *in vivo* with GRF3, as well as with chromatin-remodeling complexes, providing a mechanistic explanation for the synergistic activities of a GRF3–GIF1 complex. Interestingly, we found that, in addition to the leaf size, the GRF system also affects the organ longevity. Genetic and molecular analysis revealed that the functions of GRFs in leaf growth and senescence can be uncoupled, demonstrating that the miR396-*GRF-GIF* network impinges on different stages of leaf development. Our results integrate the post-transcriptional control of the *GRF* transcription factors with the progression of leaf development.

Keywords: miR396, growth-regulating factor, GRF-interacting factors, AN3, proliferation, senescence.

INTRODUCTION

Leaves are generated at the flanks of the shoot apical meristem. Initially a rod-shaped primordium, the developing organ grows to generate a flat lamina. At an early stage, cell proliferation occurs rapidly throughout the primordium, then it becomes restricted to the base of the organ until it finally stops rather abruptly (Donnelly *et al.*, 1999; Beemster *et al.*, 2005; Andriankaja *et al.*, 2012). Once cell proliferation has ceased, cells begin to enlarge and expansion becomes the main driver of organ growth (Cosgrove, 2005; Gonzalez *et al.*, 2012). The expanded leaf switches from a metabolic sink into a source of nutrients for the plant. In a last stage of its life, the leaf enters senescence, a complex program to recycle leaf resources that involves the decrease of photosynthesis and chlorophyll, and the final death of the leaf cells (Lim *et al.*, 2007; Breeze *et al.*, 2011).

Small RNAs in general and microRNAs (miRNAs) in particular are important regulators of different stages of leaf development, including leaf size and shape, organ polarity and senescence (Pulido and Laufs, 2010; Rubio-Somoza and Weigel, 2011). The small RNAs can also have specific patterns of expression during organ development. miRNA miR390 and ta-siRNAs are specifically expressed in the adaxial side of the leaf, while miR165/166 is active on the abaxial side (Kidner and Martienssen, 2004; Chitwood *et al.*, 2007). miRNAs are also temporarily regulated during the development of the leaf. miR164 levels decrease during maturation allowing *ORE1/AtNAC2* to be induced

(Kim *et al.*, 2009). In turn, miRNA miR396 accumulates with the age of the leaf, reducing the levels of its targets, the G*ROWTH-REGULATING FACTORs* (*GRFs*) transcription factors, whose expression remains high at early stages of leaf development (Rodriguez *et al.*, 2010; Debernardi *et al.*, 2012).

In *Arabidopsis thaliana*, the *GRF* family of transcription factors is composed of nine members (Kim *et al.*, 2003) and seven of them (*GRF1, 2, 3, 4, 7, 8, 9*) are controlled by miR396 (Jones-Rhoades and Bartel, 2004). Mutations in different *GRFs* (Kim *et al.*, 2003, 2012; Kim and Kende, 2004; Horiguchi *et al.*, 2005; Kim and Lee, 2006) or overexpression of miR396 (Liu *et al.*, 2009; Rodriguez *et al.*, 2010; Wang *et al.*, 2011) reduce the size of the leaf, indicating a partial functional redundancy. In contrast, overexpression of *GRFs* or mutating the miR396-binding box of *GRF2, GRF7* or *GRF9* generates slightly bigger leaves (Gonzalez *et al.*, 2010; Rodriguez *et al.*, 2010; Liang *et al.*, 2013).

GRF proteins physically interact with GRF-interacting factors (GIFs). Mutations in *GIF1,* also known as *ANGUSTIFOLIA3* (*AN3*), cause a reduction of leaf size (Kim and Kende, 2004; Horiguchi *et al.*, 2005) similar to the phenotypes seen in *grf* mutants or 35S:*miR396* plants. The reduction of leaf size seen in *gif1* is increased by combination with *gif2* and *gif3* (Lee *et al.*, 2009). GIF1 lacks a DNA-binding motif but shares homology to the human co-activator SYT (Kim and Kende, 2004; Horiguchi *et al.*, 2005), which is known to interact with chromatin-remodeling complexes in animals (Thaete *et al.*, 1999; Nagai *et al.*, 2001; Perani *et al.*, 2003).

Here, we found that GIF1 can interact *in planta* with both chromatin-remodeling complexes and GRF proteins, preferentially GRF3 and GRF5. Transgenic plants expressing a *GRF3* transgene insensitive to miR396 have a large increase in cell number and leaf size. Still, the effects of *GRF3* can be boosted by an additional increase of *GIF1* expression. Transcript profiling indicated that the simultaneous increase of *GRF3* and *GIF1* caused synergistic effects in gene expression, suggesting specific roles for the GRF–GIF protein complex. Analysis of the transgenic plants and mutants with altered *GRF* and *GIF* levels uncovered a function of the miR396-*GRF-GIF* network in the control of leaf longevity. Detailed molecular analysis indicated that the role of the *GRF* system in leaf size can be uncoupled from the control of leaf senescence, indicating that the GRFs affect different stages of leaf development.

RESULTS

Identification of GIF1-interacting proteins

GIF1 has been identified as the main GRF-interacting partner by yeast two-hybrid experiments (Kim and Kende, 2004; Horiguchi *et al.*, 2005). We decided to analyze, however, proteins associated with GIF1 *in planta.* To this end we made use of a transgenic line expressing a GIF1–GFP fusion protein from the *GIF1* endogenous regulatory sequences (GIF1:*GIF1-GFP,* Figure 1a). This vector fully rescued the *an3-1* mutant, which is defective in *GIF1* (Figure 1b, c), and we observed an intense GIF1–GFP signal in inflorescences (Figure 1d), in agreement with the high transcript levels of *GIF1* in these tissues as determined by the AtGenExpress atlas (Figure 1e) (Schmid *et al.*, 2005).

We immunoprecipitated the GIF1 complex using anti-GFP antibodies from inflorescences and analyzed the output by LC-MS/MS followed by label-free protein quantification analysis (Smaczniak *et al.*, 2012b). We found that proteins that were enriched in the GIF1–GFP samples fall in two different groups, GRFs and proteins involved in chromatin-remodeling processes (Jerzmanowski, 2007; Kwon and Wagner, 2007) (Table 1, for the complete data see Table S1).

Interestingly, many components necessary to generate a functional SWITCH/SUCROSE NONFERMENTING (SWI/SNF) complex were identified in our pull downs (Table 1), including three different ATPases of the SWI/SNF family: BRAHMA (BRM), SPLAYED (SYD) and CHR12; and additional subunits of the complex, SWP73A (SWI/SNF ASSOCIATED PROTEIN 73A) and ARP7 (ACTIN RELATED PROTEIN 7) (Jerzmanowski, 2007; Kwon and Wagner, 2007). Similar results have been recently found in Arabidopsis cell cultures and seedlings (Vercruyssen *et al.*, 2014).

It has been already pointed out that the N-terminal domain of GIF1 has homology with the SNH domain of the human co-activator SYT (Kim and Kende, 2004), which in turn mediates the interaction with human SWI/SNF ATPases (Thaete *et al.*, 1999). Our data are consistent with these observations and point towards a similar function of Arabidopsis GIF1 and human SYT in the recruitment of chromatin remodelers.

On the other hand, we found that GIF1 mainly interacted with two GRFs in our system, GRF5 and GRF3 (Table 1 and Figure 1e). The AtGenExpress atlas showed that *GIF1, GRF3* and *GRF5* are co-expressed in many samples with the highest transcript levels in developing organs (Figure 1e). The pattern of the SWI/SNF ATPases was more homogenous in the different samples (Figure 1f), which might be expected from their different biological functions that go beyond the GRF–GIF system (Jerzmanowski, 2007; Kwon and Wagner, 2007).

Role of the miR396-GRF3 node during leaf development

Interestingly, the two GRFs detected as GIF1 partners by our system, GRF3 and GRF5 are differentially affected by miR396. On the one hand, *GRF3* has a miR396-binding site and is post-transcriptionally repressed by miR396 (Rodriguez *et al.*, 2010). On the other hand, *GRF5* lacks a miR396 target site and therefore it is not regulated by this

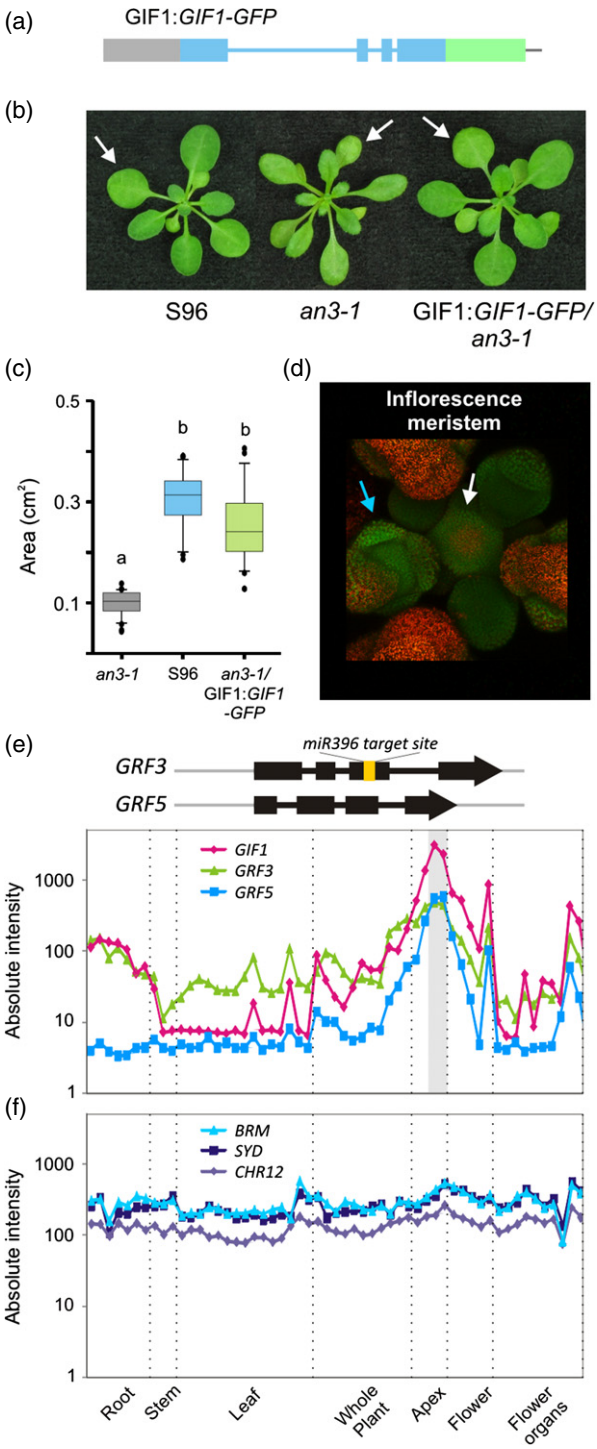

Figure 1. Functional complementation of *an3-1* mutants by GIF1:*GIF1-GFP*.
(a) Scheme showing the vector expressing *GIF1* from its own promoter (grey box) fused to *GFP* (green box).
(b, c) Rosettes and area of the first pair of leaves of wild-type (S96) and *GIF1* mutants (*an3-1*) expressing or not GIF1:*GIF1-GFP*. Data from *an3-1*/GIF1:*GIF1-GFP* leaves correspond to different primary transgenic plants ($n = 15$). [a,b]Different letters indicate significant differences as determined by one-way rank-based analysis of variance (ANOVA) followed by Dunn's test ($P < 0.05$). The GIF1:*GIF1-GFP* construct was able to complement *an3-1*. White arrows indicate the first leaves.
(d) GIF1:*GIF1-GFP* expression in inflorescences under confocal microscopy. White arrow indicates meristem, while the light blue arrow indicates a flower primordium.
(e, f) Expression profile of *GIF1* and genes encoding GIF1 interactors. Data obtained from AtGenExpress corresponding to Col-0 samples (Schmid *et al.*, 2005). (e) *GIF1, GRF3* and *GRF5*. The grey bar highlights inflorescence meristem samples. *GRF3* and *GRF5* genes are represented with black boxes and lines corresponding to exons and introns, respectively. An orange box shows the miR396 target site in *GRF3*. (f) SWI/SNF ATPases: *BRAHMA, SPLAYED* and *CHR12*.

miRNA (Figure 1e). As the role of *GRF5* in the control of cell proliferation in leaves has been previously studied (Horiguchi *et al.*, 2005; Gonzalez *et al.*, 2010), we decided to focus on *GRF3,* which is additionally controlled at the post-transcriptional level by miR396.

To investigate the function of *GRF3* in leaf growth we first characterized a homozygous T-DNA insertional mutant on a Columbia background (*Salk026786,* named *grf3-1*) that caused a five-fold reduction in *GRF3* transcript levels with respect to wild-type plants (Figure 2a). We measured the area of the first pair of leaves of this mutant together with a mutant for *GRF5* (*grf5-1*) and plants overexpressing miR396b (Figure 2a). The *grf3-1* mutant had smaller leaves than wild-type, approximately 15% (Figure 2a). The reduction in leaf size was similar to that of *grf5-1,* which has been previously reported (Horiguchi *et al.*, 2005). Plants harboring 35S*:miR396b* have a stronger reduction in leaf size as expected from a reduced expression of several *GRFs* with redundant function (Figure 2a).

Then we studied the regulation of *GRF3* by miR396 and generated transgenic plants that express a mutated version

Table 1 GIF1 interacting proteins

GIF1:*GIF1-GFP*–IP–LC-MS/MS		
Protein		Log2PER[a]
At3g13960	GRF5	7.60
At5g28640	GIF1	6.45
At2g36400	GRF3	4.22
Chromatin remodelers[b]		Log2PER[a]
At2g46020	BRAHMA	4.87
At3g60830	ARP7	3.29
At3g06010	CHR12	3.22
AT5G58230	MSI1	2.87
At5g14170	SWP73B	2.67
At2g28290	SPLAYED	2.32
At5g44800	CHR4	1.37

[a]Log2 protein enrichment ratio: protein enrichment values with significant differences at a false discovery rate (FDR) 0.05 with respect to plants without the transgene.
[b]A light blue box highlights components of the SWI/SNF chromatin-remodeling complexes.

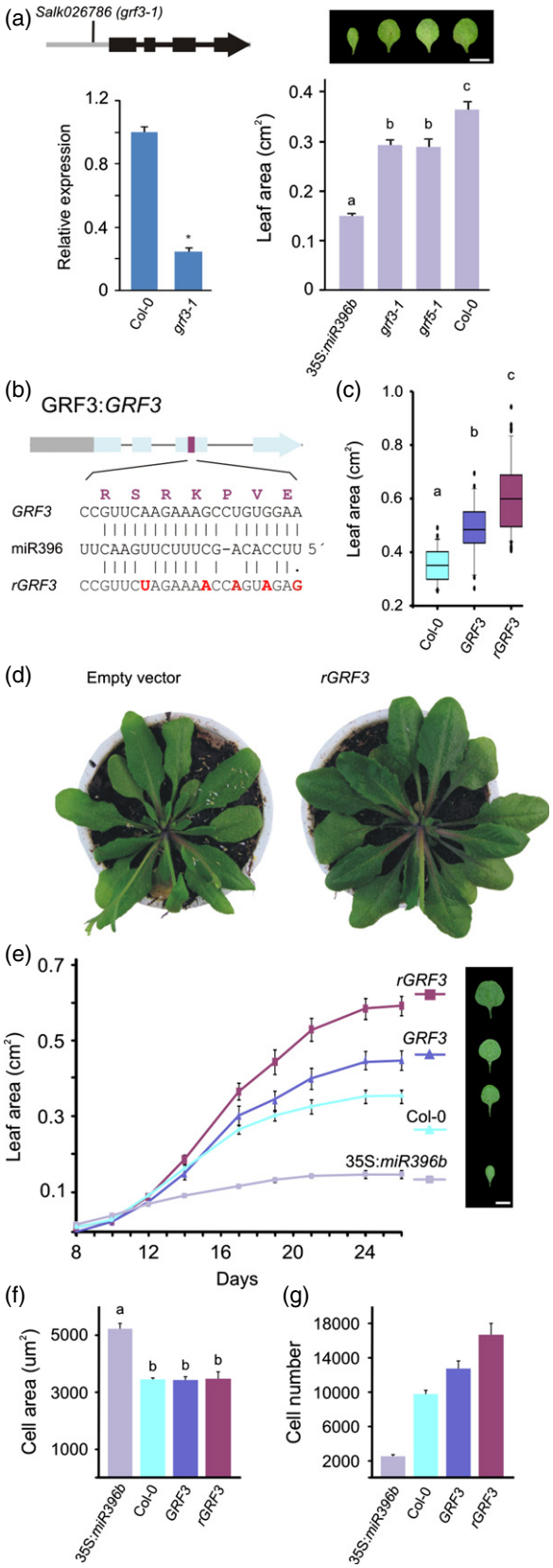

Figure 2. Control of leaf growth by the miR396-*GRF3* node.
(a) Left, scheme of *GRF3* indicating the position of the *Salk026786* insertion (*grf3-1*) and *GRF3* expression level determined by RT-qPCR. Expression levels were normalized to wild-type plants. Data shown are mean ± standard error of the mean (SEM) of three biological replicates. Right: Area and pictures of fully expanded first leaves of *grf3-1, grf5-1,* 35S:*miR396b* and wild-type plants of 4 weeks. Scale bar: 0.5 cm.
(b) Scheme showing two *GRF3* expression vectors. *GRF3* represents the wild-type gene including the promoter region, while *rGRF3* harbours point mutations that diminish the interaction with miR396 but not affect the amino acid sequence.
(c) Area of fully expanded first leaves of independent primary transgenic plants expressing *GRF3* or *rGRF3* from its own regulatory regions. At least 50 primary transgenic plants were analyzed in each case.
(d) Representative rosettes of wild-type plants transformed with an empty vector and *rGRF3*.
(e) Growth of the first leaves in wild-type (Col-0) plants, and stable transgenic plants harboring 35S:*miR396b, GRF3* and *rGRF3* transgenes. Days: days after sowing. See Figure S1(a) for *GRF3* transcript levels in the different plants. Scale bar: 0.5 cm.
(f, g) Cell area (f) and estimated cell number (g) in fully expanded first leaves (4 weeks after germination) of the different transgenic plants used in (e).
Asterisks indicate values significantly different from Col-0 as determined by Student's *t*-test ($P < 0.05$).;
[a–c]Different letters indicate significant differences as determined by one-way analysis of variance (ANOVA) followed by Tukey's test ($P < 0.05$).

of *GRF3* insensitive to miR396 regulation under its own promoter (*rGRF3*). The mutations introduced did not change the amino acid sequence, but altered the miR396 complementary site in order to abolish the miRNA interaction (Figure 2b). As a control, we used a similar vector expressing a wild-type *GRF3* gene (*GRF3*).

We observed that *rGRF3* primary transgenic plants were bigger than control plants (Figure 2c, d). The first leaves of *rGRF3* plants had an increase in their size of more than 70% with respect to an empty vector (Figure 2c, e). Interestingly, the increase of leaf size caused by *rGRF3* was larger than that reported previously for other *GRFs,* such as *rGRF2, rGRF7* and *rGRF9* (Rodriguez *et al.*, 2010; Wang *et al.*, 2011; Liang *et al.*, 2013).

We then characterized in more detail the growth of the first pair of leaves harboring different alleles of *GRF3* (Figures 2e and S1a). Initially, leaves of *rGRF3* and control lines grew at the same rate (Figure 2e). However, after 12 days the growth rate of control plants began to decrease, whereas *rGRF3* leaves continued to grow. As a result of this extended period of growth, the leaf blade of *rGRF3* almost doubled those of wild-type plants (Figure 2e). Leaves of transgenic plants harboring an extra copy of a wild-type *GRF3* gene were slightly bigger than the control, while plants ectopically expressing miR396 had smaller leaves, as expected (Figure 2e). The cell size in fully expanded leaves was unaffected by the presence of *rGRF3* (Figure 2f) showing that *rGRF3* increases the number of cells in leaves (Figure 2g). Altogether, these results show the capacity of *GRF3* to increase the leaf size in Arabidopsis, specifically when decoupled from the regulation by miR396.

Stimulation of GRF3 activity by GIF1

The previous results showed an increase in cell number in Arabidopsis leaves by *rGRF3*. Considering that GRFs can work in concert with GIF1 we decided to test whether this increase in leaf size by *rGRF3* reached a maximum or it could be further modulated by changing *GIF1* levels. To do this, we first generated Arabidopsis plants expressing 35S:*GIF1* (Figures 3a and S1b). The first leaves of these plants showed a slight increase in leaf area, which was not statistically significant in our experimental conditions (Figure 3a, b).

Interestingly, co-expression of 35S:*GIF1* and *rGRF3* caused a clear increase in leaf size in addition to the effects of *rGRF3* alone (Figure 3a, b). We found that *rGRF3* increases the size of the first pair of leaves 1.7 times with respect to wild-type, while the simultaneous expression of *rGRF3* and 35S:*GIF1* generated a 2.3-fold increase (Figure 3a, b). Cells of *rGRF3x*35S:*GIF1* had a final size similar to cells of the control plants (Figure 3c), so that GIF1 enhanced the activity of GRF3 and additional increase the number of cells in leaves harboring a *rGRF3* transgene (Figure 3d). We also evaluated the effects caused by the simultaneous overexpression of *GIF1* and *GRF5,* the other GRF detected as a GIF1 partner in our approach. As *GRF5* is not regulated by miR396, we made used of a 35S:*GRF5* line described previously that expresses the transcription factor from the strong *35S* viral promoter (Horiguchi *et al.*, 2005; Gonzalez *et al.*, 2010). Co-overexpression of *GRF5* and *GIF1* also caused an additional increase in leaf size compared with the single overexpressing lines (Figure S2a, c). However, we observed a more limited effect of *GRF5* than the miR396-regulated *GRF3.*

To further study the interaction between *GIF1* and *GRF3* we analyzed the effect of the expression of *rGRF3* in plants deficient in *GIF1.* The *an3-1* mutant (S96 ecotype), lacks *GIF1* activity and therefore has smaller leaves (Horiguchi *et al.*, 2005) (Figure 3e). We introduced a *rGRF3* transgene in *an3-1* and observed a partial complementation of the leaf size phenotype, being two times larger than the leaves of the single mutants, but still smaller than wild-type (Figure 3e, f, h; see Figure S3a for data with primary transgenic plants). We observed a similar effect when *GRF5* was overexpressed in the *an3-4* mutant (Figure S2b). Furthermore, cells of *rGRF3/an3-1* are larger than wild-type (Figure 3g) and similar to *an3-1*. The larger size of *an3-1* cells has been noted before as part of a compensation process to maintain the size of the organ (Tsukaya, 2005; Kawade *et al.*, 2010; Horiguchi and Tsukaya, 2011). These results indicate that *rGRF3* can increase leaf size in the absence of *GIF1* albeit it cannot fully recover the wild-type levels.

Regulation of gene expression by GRF3-GIF1 complexes

The synergistic increase in leaf size of the *rGRF3x*35S:*GIF1* plants suggested that GIF1 stimulates the activity of GRF3.

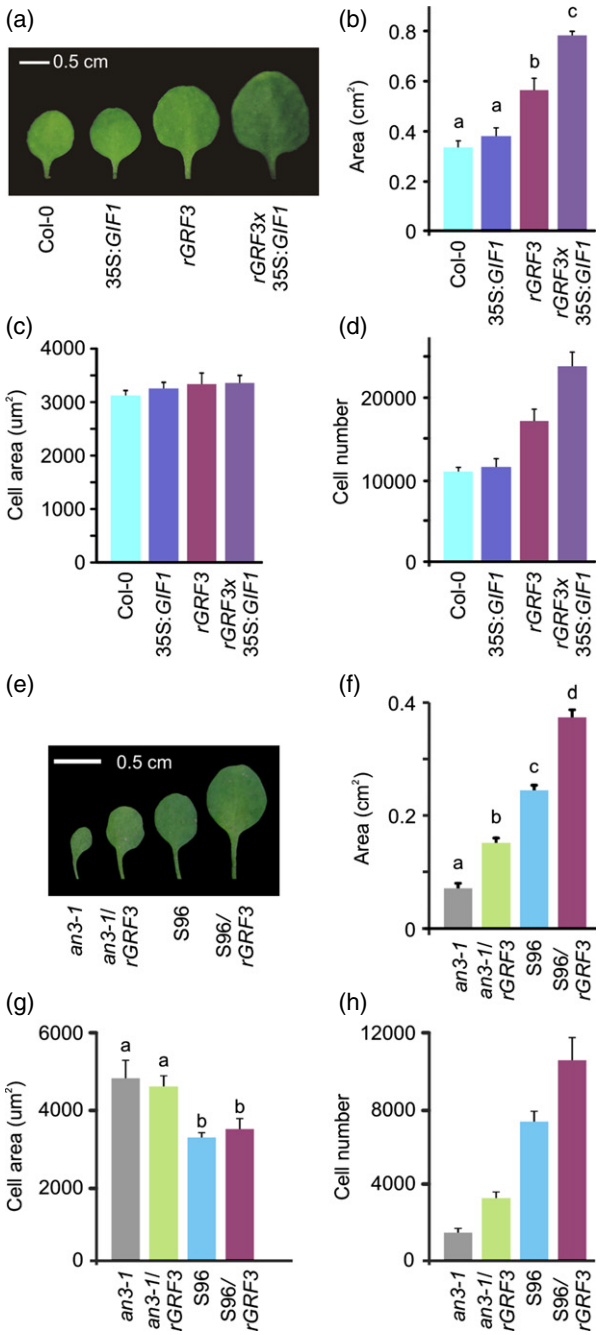

Figure 3. Genetic interaction between *GIF1* and *GRF3.*

(a, b) Pictures (a) and area (b) of fully expanded first leaves of wild-type and 35S:*GIF1, rGRF3* or *rGRF3x*35S:*GIF1* plants. See Figure S1(b) for *GRF3* and *GIF1* transcript levels in the different plants. Data shown are mean ± standard error of the mean (SEM) ($n = 20$).

(c, d) Cell area (c) and estimation of cell number (d) of fully expanded first leaves of wild-type and 35S:*GIF1, rGRF3* or *rGRF3x*35S:*GIF1* plants.

(e, f) Pictures (e) and area (f) of fully expanded first leaves of *an3-1,* wild-type (S96) and T2 *an3-1/rGRF3* and S96/*rGRF3* plants. See Figure S3(c) for *GRF3* and *GIF1* transcript levels in the different plants. Data shown are mean ± SEM ($n = 20$).

(g, h) Cell area (g) and estimation of cell number (h) of fully expanded first leaves of *an3-1,* wild-type (S96), *an3-1/rGRF3* and S96/*rGRF3* plants.

[a–d]Different letters indicate significant differences as determined by one-way analysis of variance (ANOVA) followed by Tukey's test ($P < 0.05$).

Therefore, we analyzed the expression of cell proliferation markers, *CYCLINB1;1, CYCLIND3;1* and *KNOLLE*. In shoot apices of 10-day-old seedlings, the expression levels of the cell proliferation markers were similar in all the samples (Figure 4a). We next analyzed these markers in the first pair of leaves in seedlings of the same age (note that at this time leaves are actively growing, see Figure 2e). In this case we observed that the transcript levels of *KNOLLE* and *CYCLINB1;1* in *rGRF3x*35S:*GIF1* leaves were at least two-fold higher than in wild-type plants (Figure 4a). In this sample, the proliferation markers were also slightly higher in *rGRF3* plants (approximately 1.5-fold for *KNOLLE*) (Figure 4a). Therefore, the larger leaves with more cells of *rGRF3x*35S:*GIF1* plants correlate with a significant increase in the expression of cell proliferation markers in developing young leaves.

Next, we compared the transcriptome of 35S:*GIF1, rGRF3* and *rGRF3x*35S:*GIF1* plants, using ATH1 Affymetrix microarrays (Data S1). For these experiments we collected vegetative apices together with the leaf primordia. We took a young tissue to minimize potential secondary effects that might be caused by the prolonged expression of these transgenes. We selected genes with increased transcript levels in each genotype with respect to wild-type plants (note that we have performed two replicates per sample and also requested at least a 1.5-fold change with respect

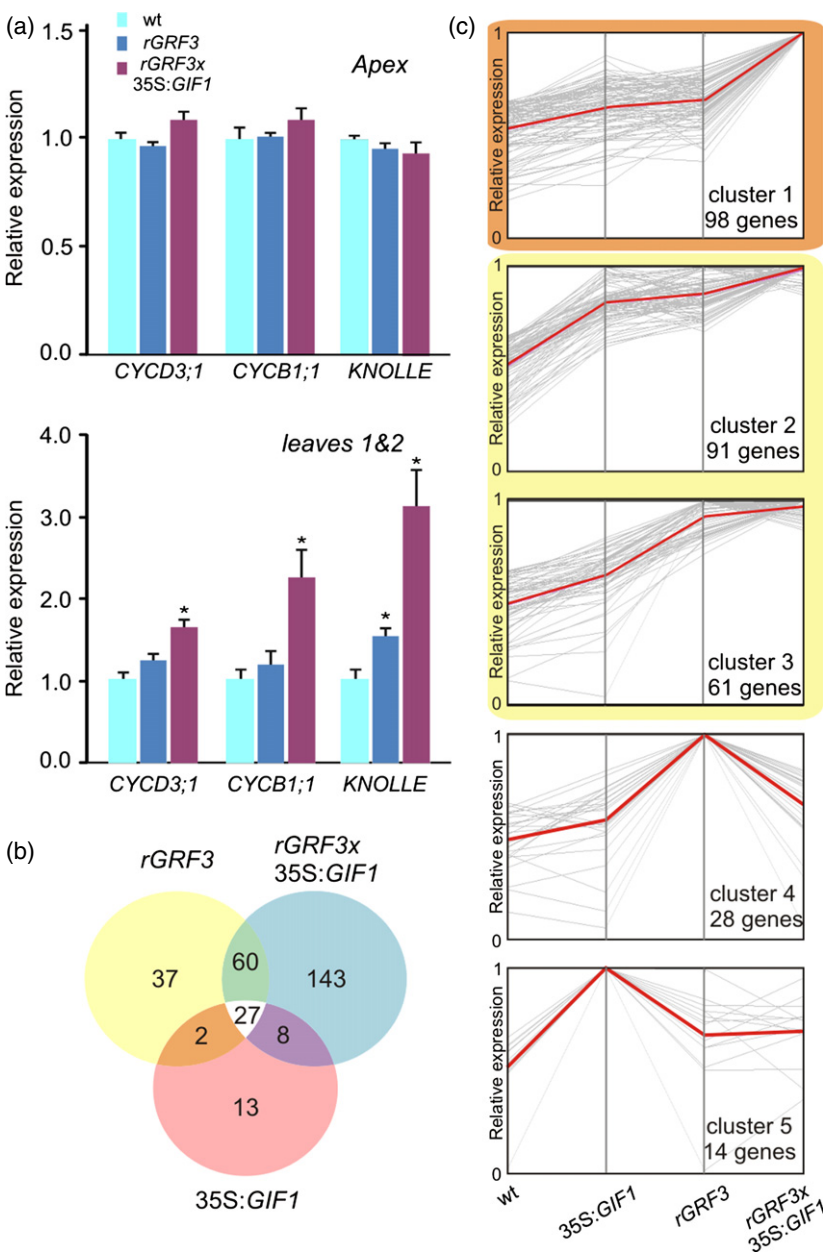

Figure 4. Transcriptional responses to *rGRF3* and 35S:*GIF1*.
(a) *CYCD3;1, CYCB1;1 and KNOLLE* transcript levels estimated by RT-qPCR in the first pair of leaves and apices of 10 day-old wild-type (wt), *rGRF3* and *rGRF3x*35:*GIF1* seedlings. Expression levels were normalized to wild-type levels. Data shown are mean ± standard error of the mean (SEM) of three biological replicates. Asterisks mean statistically different from wt as determined by Student's *t*-test ($P < 0.05$).
(b) Genes induced by *rGRF3,* 35S:*GIF1* and *rGRF3x*35S:*GIF1* (two biological replicates per sample, 1.5-fold change and $P < 0.05$, see Experimental Procedures for details).
(c) Genes with increased expression in *rGRF3,* 35S:*GIF1* and *rGRF3x*35S:*GIF1* (b) were clustered according to their expression pattern (see Experimental Procedures for details).

to wild-type, see Experimental Procedures for details) (Figure 4b; see Figure S4 for the genes with reduced transcript levels in these samples).

In total, we found 292 genes with increased transcript levels in any of the transgenic plants (Figure 4b). *rGRF3x*35S:*GIF1* plants had the highest number of induced genes, 238, and 143 out of them were only detected in this sample (Figure 4b), in agreement with a hyper-activation of GRF3 in the presence of GIF1. We observed that five clusters described the tendencies of most of the 292 induced genes (see the average of each cluster in red, Figure 4c). The largest cluster contained 98 genes (Cluster 1), and included genes that respond mostly to the GRF3-GIF1 complex rather than the individual transgenes (Figure 4c). *MYB3R3,* one of the five Arabidopsis R1R2R3-Myb transcription factors known to bind to the promoters of mitosis specific genes (Haga *et al.*, 2007) was found in this cluster. GO term enrichment analysis (Brady *et al.*, 2007) showed that many protein kinases were also induced in *rGRF3x*35S:*GIF1* plants (Table S2).

Cluster 2 (91 genes) and cluster 3 (61 genes) included genes that responded to *rGRF3x*35S:*GIF1* and also to *rGRF3* and/or 35S:*GIF1* individual transgenes, respectively. Clusters 4 (28 genes) and 5 (14 genes) contained fewer genes that responded mostly to one of the individual transgenes. Altogether, the transcriptome analysis suggests that plants expressing high levels of GRF3–GIF1 complexes show a global response including that of *rGRF3* or 35S:*GIF1,* with an additional over-activation of a specific group of genes. These effects are consistent with the synergistic increase of leaf size observed in *rGRF3x*35S:*GIF1* plants.

Control of leaf senescence by GRF transcription factors

While growing the different transgenic lines we noticed that in addition to the effects on leaf size, *rGRF3* and *rGRF3x*35S:*GIF1* caused an obvious delay of leaf senescence. Sixty-day-old Arabidopsis plants (Col-0) display visual signs of senescence including yellowish leaves (Figure 5a). In contrast, leaves of plants harboring *rGRF3* were still green and turgid. Interestingly, while 35S:*GIF1* did not display obvious signs of delayed senescence *per se,* high levels of *GIF1* enhanced the effects caused by *rGRF3* alone (Figure 5a), resembling the previous results in leaf size. We also observed that plants overexpressing *GRF5* have an obvious delay in senescence (Figure S5a).

So far, the GRF transcription factor family and their co-regulator GIF1 have been widely associated with the control of leaf size (Kim *et al.*, 2003; Kim and Kende, 2004; Horiguchi *et al.*, 2005; Liu *et al.*, 2009; Rodriguez *et al.*, 2010; Wang *et al.*, 2011; Debernardi *et al.*, 2012; Mecchia *et al.*, 2013). Our results suggest that the GRFs have functions in plant development that might go beyond organ size control.

Several plant hormones are known to affect leaf senescence [reviewed in (Lim *et al.*, 2007)]. Therefore, we analyzed the expression of genes that have been shown to respond to hormones (Nemhauser *et al.*, 2006) in our microarray experiment, but we did not find any obvious connections (Figure S6).

We next studied the role of the *GRFs* in leaf senescence in more detail. To quantify the effects we turned to another approach using dark-induced senescence of detached leaves and followed the process by measuring the photochemical efficiency (Fv/Fm) of Photosystem II (PSII) (Oh *et al.*, 1997). We observed that *rGRF3* caused a delay of senescence also in this system: wild-type and 35S:*GIF1* leaves senesced 8 days after detaching, whereas *rGRF3* did 12 days after detaching (Figure 5b). In the same conditions, *rGRF3x*35S:*GIF1* leaves senesced 14 days after detaching, showing again the capacity of GIF1 to stimulate the effects of GRF3.

Considering the phenotypes of plants that harbor a miRNA-insensitive *GRF3* (with or without *GIF1*) or overexpress *GRF5,* we analyzed plants with reduced levels or loss-of-function mutations in *GRF3* and *GRF5.* In agreement, we observed that plants overexpressing miR396 senesced significantly faster than wild-type (Figure 5b). We also observed that *grf3*-1 and *grf5*-1 mutants displayed a mild acceleration of the senescence program (Figure S5b). Together, the results indicate a redundant role of GRFs in the control of leaf longevity during normal leaf development.

It is known that several genes are induced during dark-induced senescence, like *SEN1, SEN4* and *SAG12* (Oh *et al.*, 1996; Park *et al.*, 1998; Noh and Amasino, 1999). The level of these genes was evaluated by quantitative reverse transcription polymerase chain reaction (RT-qPCR) in detached leaves at different days, where senescence was induced by darkness. *SEN1* and *SEN4* levels increased at 2 days after incubation in wild-type plants, and this increase was higher at 4 days (Figure 5c). *SAG12* level was strongly increased at the fourth day after incubation (Figure 5c). We observed a greater induction of the markers *SEN1* and *SEN4* in 35S:*miR396* plants (Figure 5c). On the other hand, we observed that in *rGRF3* leaves there was no significant induction of any of these genes at 4 days after detaching (Figure 5c). These quantitative results on expression of specific markers of leaf senescence are in agreement with our data supporting a previously unnoticed role of the miR396-*GRF-GIF* module in the control of leaf senescence.

Finally, we tested the interaction between *rGRF3* and *an3-1* during leaf senescence. We found that the *an3-1* mutant also has an accelerated senescence (Figure 5d, e), as expected from our previous data. In both experimental systems, dark-induced leaf senescence and whole plants, *rGRF3* delayed the senescence of *an3-1* leaves (Figure 5d,

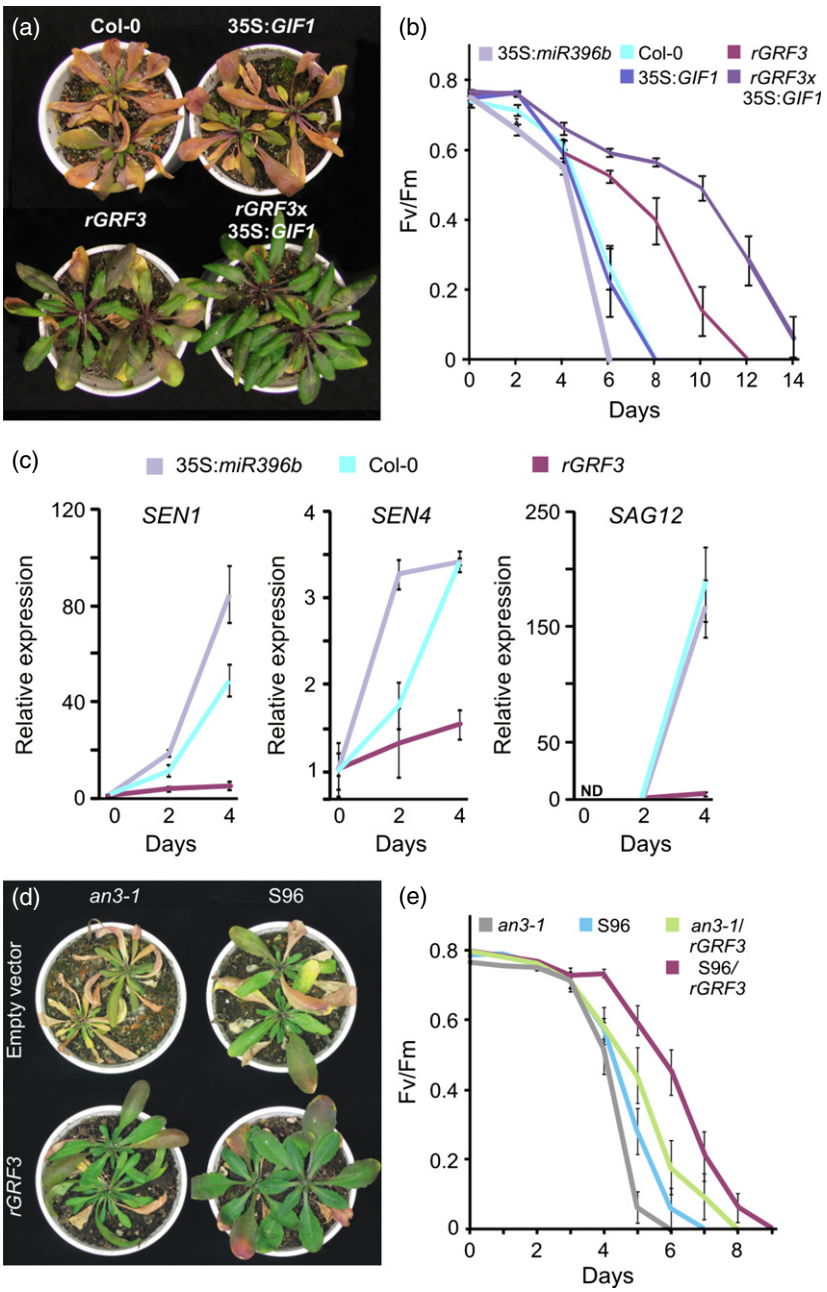

Figure 5. Role of the miR396-*GRF3-GIF1* node in the control of leaf senescence.
(a) Rosette plants (60-day-old) of wild-type (Col-0) and 35S:*GIF1*, *rGRF3* or *rGRF3x*35S:*GIF1*. The inflorescence stems were removed to show the rosette leaves.
(b) Measurements of photochemical efficiency (Fv/Fm) of PSII in detached fifth leaves incubated in the dark of wild-type and 35S:*miR396*, 35S:*GIF1*, *rGRF3* or *rGRF3x*35S:*GIF1* lines. Data shown are mean ± standard error of the mean (SEM) of 12 biological replicates.
(c) *SEN1*, *SEN4 and SAG12* transcript levels estimated by RT-qPCR in detached fifth leaves incubated in dark for 2 or 4 days. Leaves of wild-type plants, and of plants harboring 35S:*miR396* or *rGRF3* transgenes were analyzed. Data shown are mean ± SEM of three biological replicates.
(d) Pictures of 40-day-old rosettes of *an3*-1, wild-type (S96) and T2 *an3-1*/*rGRF3* and S96/*rGRF3* plants. See Figure S3(c) for *GRF3* and *GIF1* transcript levels in the different plants.
(e) Measurements of photochemical efficiency (Fv/Fm) of PSII in detached fifth leaves incubated in dark of *an3*-1, wild-type (S96), *an3-1*/*rGRF3* and S96/*rGRF3* plants. Data shown are mean ± SEM of 12 biological replicates.

e; see Figure S3b for data with primary transgenic plants). Interestingly, while *rGRF3* could not fully recover the organ size of *an3-1*; *rGRF3/an3-1* leaves have a delayed senescence with respect to the wild-type. That the smaller leaves of *rGRF3*/*an3-1* plants senescence later than wild-type suggested that the delay in senescence is not the simple secondary consequence of the increase in leaf size by *rGRF3.*

Uncoupling *rGRF3* functions in leaf size and senescence

Our results showed that *rGRF3* increases the cell number of the leaves and generates larger organs. Therefore, it might be argued that the increase in leaf longevity could be a consequence of a prolonged proliferative phase caused by *rGRF3* or, alternatively, it could reflect an additional function of this transcription factor. To distinguish between these possibilities, we expressed *rGRF3* in a temporally controlled way during leaf development.

First, we generated a GRF3:*GUS* reporter and found that the promoter of *GRF3* was active constitutively during leaf development (Figure 6a). We concluded then that the GRF3:*rGRF3* transgene drives the expression of the transcription factor in a broad domain during leaf development, as it evades the post-transcriptional regulation guided by miR396, as was reported for *GRF2* (Rodriguez

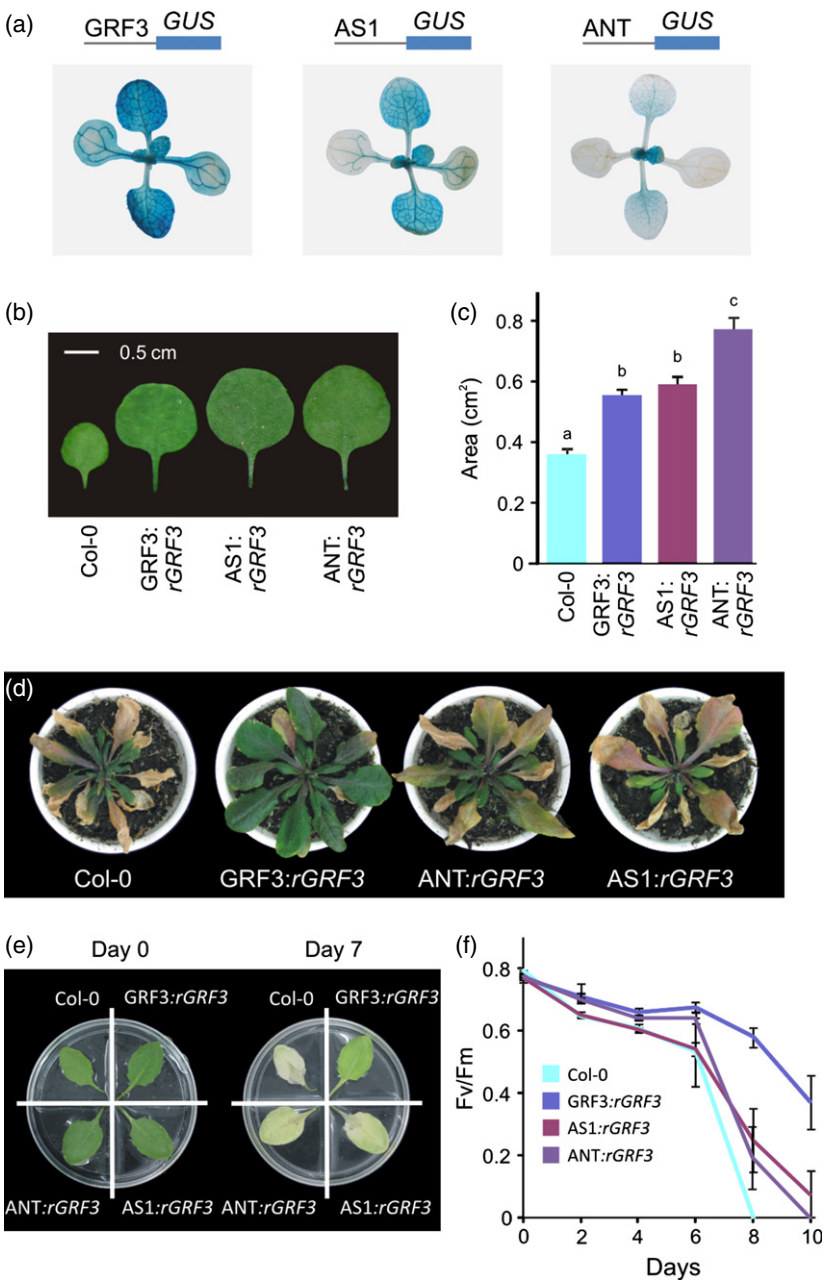

Figure 6. Uncoupling *rGRF3* functions in leaf size and senescence.
(a) GUS staining of representative GRF3:*GUS* (left), AS1:*GUS* (middle) and ANT:*GUS* (right) reporters (15-day-old plants). Above: Scheme representing the reporters.
(b, c) Pictures (b) and area (c) of full-expanded first leaves of Col-0, *rGRF3* (GRF3:*rGRF3*), AS1:*rGRF3* and ANT:*rGRF3* plants. Data shown are mean ± standard error of the mean (SEM) ($n = 20$). Different letters indicate significant differences as determined by one-way rank-based analysis of variance (ANOVA) followed by Tukey's test ($P < 0.05$).
(d) Pictures of 50-day-old rosettes.
(e, f) Pictures of fifth leaves after detaching (0 and 7 days) (e) and measurements of photochemical efficiency (Fv/Fm) (f) of PSII in the detached leaves. Data shown are mean ± SEM of 12 biological replicates.

et al., 2010). We decided next to restrict *rGRF3* to younger leaf stages by expressing it from the *ASSYMETRIC LEAVES1* (*AS1*) and *ANTEGUMENTA* (*ANT*) promoters (Figure 6a) (Wang *et al.*, 2009).

We obtained *rGRF3* (GRF3:*rGRF3*), AS1:*rGRF3* and ANT:*rGRF3* transgenic plants expressing similar levels of *GRF3* in apices of 10-day-old seedlings (Figure S7a). Analysis of AS1:*rGRF3* and ANT:*rGRF3* first leaves size showed that these plants had a significant increase in leaf area with respect to wild-type plants, 1.7 and 2.2 times respectively (Figures 6b, c and S7b). Therefore, *rGRF3* expressed from its own regulatory regions and AS1:*rGRF3* caused similar increases in leaf size, while ANT:*rGRF3* was even stronger (Figures 6b, c and S7b), indicating that the specific expression pattern of *GRF3* during early leaf development is sufficient to further increase leaf size. We also confirmed that the area of the cells were unchanged (Figure S7c), meaning that the increase in leaf area was due to a higher cell number.

Then we analyzed senescence phenotypes of whole plants (Figure 6d) and dark-induced leaf senescence (Figure 6e, f). In both assays ANT:*rGRF3,* AS1:*rGRF3* and wild-type leaves senesce rather similarly, even though their ample difference in leaf size (Figure 6d–f). In contrast,

rGRF3 expressed from its own regulatory regions caused a significant senescence delay, as expected (Figure 6d–f). Therefore, the results show that the increase in cell number and the delay in senescence caused by *rGRF3* can be uncoupled by controlling the timing of *GRF3* expression, and that GRF3 has activities that influence leaf development that go beyond the control of organ size.

DISCUSSION

Control of different stages of leaf development by GRF transcription factors

The GRF transcription factors and their co-regulators, GIFs, are well-known for their role in the regulation of cell proliferation and leaf size (Kim *et al.*, 2003; Kim and Kende, 2004; Kozuka *et al.*, 2005; Lee *et al.*, 2009; Gonzalez *et al.*, 2010; Kawade *et al.*, 2010; Rodriguez *et al.*, 2010; Horiguchi *et al.*, 2011; Wang *et al.*, 2011; Debernardi *et al.*, 2012; Mecchia *et al.*, 2013). Here, we found that they also affect later stages of the organ development and control the leaf longevity (Figure 7).

The ability to affect both the size and the longevity of the leaves has been described in other cases. For instance, plants overexpressing miRNA miR319 (Schommer *et al.*, 2008) or loss-of-function mutants in *AUXIN RESPONSE FACTOR 2* (*ARF2*) (Ellis *et al.*, 2005; Okushima *et al.*, 2005; Schruff *et al.*, 2006; Lim *et al.*, 2010) generate bigger leaves that senesce later. *ARF2,* like *rGRF3,* prolongs the expression of *CYCD3;1* in developing leaves (Ellis *et al.*, 2005), while delaying the expression of *SAG12* and *SEN4* in leaves under senescing conditions (Ellis *et al.*, 2005; Lim *et al.*, 2010). It would be interesting to test if the functions of miR319 and *ARF2* in the control of leaf growth and longevity can be uncoupled as we observed for the miR396-*GRF* system by controlling their tissue and developmental timing of expression.

Co-ordination of leaf size and longevity

Our results show that the effects caused by GRF system on leaf senescence are not a simple consequence derived from the modification of the proliferative phase of the organ. First, leaves of *an3-1* mutants expressing *rGRF3* have fewer cells than wild-type, but they senesce later. Although we have observed that GIF1 enhances the activity of GRF3 in the control of both leaf size and longevity, it might be argued that without the aid of GIF1, *rGRF3* alone has a greater effect on leaf longevity than on leaf size. Second, expression of *rGRF3* in a small temporal window during early leaf development modifies the organ size with little effect on its senescence. Therefore, during early leaf development the GRFs may stimulate cell proliferation, while a further expansion of the GRF expression domain contributes to an increased leaf longevity.

The heterochronic miR156 accumulates with the age of the plant and regulates the level of *SPL* transcription factors, which in turn decide the transition from the juvenile to adult phase of the plant (Wu and Poethig, 2006; Wang *et al.*, 2009; Wu *et al.*, 2009). It has been shown that miR396 accumulates steadily during the development of each leaf, even beyond the cell proliferation phase (Rodriguez *et al.*, 2010). In this context, miR396 levels could serve as a marker determining both the duration of the proliferative phase and the longevity of each organ (Figure 7), in an analogous way miR156 is correlated with the age of the whole plant.

It remains to be determined how GRFs transcription factor mediate the effects on leaf size and longevity. Our microarray data suggested no obvious connections to hormone pathways. Similar results were obtained for 35S:*GRF5* plants (Gonzalez *et al.*, 2010), however we cannot discard a direct connection to hormone pathways in other development stages.

GIF1 as a GRF co-regulator

The GRF transcription factors contain two conserved domains: QLQ which mediates the interaction with GIF1, and WRC which binds to DNA (Kim *et al.*, 2003, 2012; Horiguchi *et al.*, 2005). In contrast, GIFs lack a DNA-binding domain, but contain an N-terminal region with homology with the SNH domain of the human co-activator SYT (Kim and Kende, 2004; Horiguchi *et al.*, 2005). The later domain mediates the interaction between SYT and the human SWI/SNF ATPases (Thaete *et al.*, 1999). In addition to the GRFs, we observed that GIF1 interacted with Arabidopsis SWI/SNF ATPases. Similar interacting partners of GIF1 were identified in a different system using a Tandem Affinity

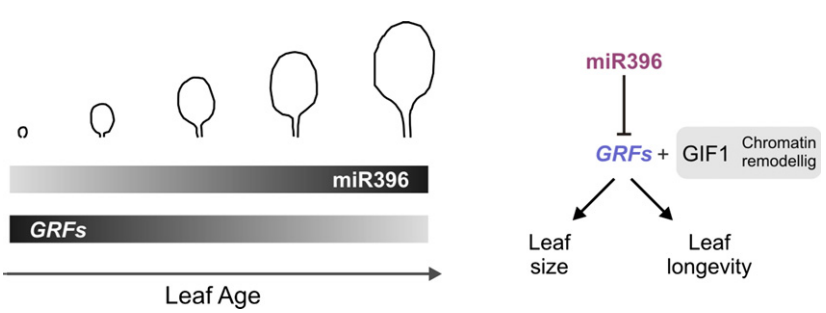

Figure 7. Control of leaf development by miR396 and growth-regulating factors (GRFs). Changes in expression level during leaf development are showed by the shaded bars. The miR396 accumulates steadily during the development of the leaf antagonizing the expression of *GRFs*. We suggest that miR396 levels could serve as a marker to determine the duration of the proliferative phase and the longevity of each organ.

Purification (TAP) approach (Van Leene *et al.*, 2007, 2008) in seedlings and cultured cells (Vercruyssen *et al.*, 2014). The findings that GIF1 interacts with SWI/SNF chromatin-remodeling proteins suggest that SYT and GIF have similar functions as co-transcription factors in animals and plants, respectively.

The interaction between GIF1 and any of the three Arabidopsis SNF/SWI ATPases (BRM, SYD and CHR12) also provides a mechanistic explanation to the function of GIF1 as a co-regulator *in vivo.* The additional effects observed in the transcript profiling of *rGRF3x*35S*:GIF1* compared with the individual transgenes is also consistent with this hypothesis. In this context, GRF3 might exert certain activity as a transcription factor *per se,* but the simultaneous expression with *GIF1* provides the complex with additional activity probably due to the capability to recruit the chromatin-remodeling complexes.

In Arabidopsis, SWI/SNF complexes affect plant growth and mutations in many of their components generate dwarf plants (Wagner and Meyerowitz, 2002; Farrona *et al.*, 2004; Sarnowski *et al.*, 2005; Hurtado *et al.*, 2006; Kwon *et al.*, 2006; Bezhani *et al.*, 2007; Jerzmanowski, 2007; Kwon and Wagner, 2007; Archacki *et al.*, 2009), which is in agreement with the functions of the GRF-GIF complex in the promotion of leaf growth. However, the SWI/SNF complexes can interact with different transcription factors (Smaczniak *et al.*, 2012a; Wu *et al.*, 2012; Efroni *et al.*, 2013) and therefore have functions that go beyond the GRF/GIF networks.

Function and regulation of the GRF transcription factors

Arabidopsis thaliana contains nine *GRF* genes (Kim *et al.*, 2003). Analysis of *GRF* mutants and miR396 overexpressors indicates that they fulfill redundant functions in the control of leaf size (this work) (Kim *et al.*, 2003; Horiguchi *et al.*, 2005; Kim and Lee, 2006; Liu *et al.*, 2009; Rodriguez *et al.*, 2010; Wang *et al.*, 2011). These results do not invalidate that certain GRFs might have specific functions. For example, GRF7 is the only GRF able to bind the *DREB2A* promoter in yeast one-hybrid experiments and it has been shown to control osmotic responding genes (Kim *et al.*, 2012). Furthermore, several GRFs have been recently shown to repress KNOX transcription factors (Kuijt *et al.*, 2014). GRF9 is also unusual as it has a duplication of the WRC domain (Kim *et al.*, 2003; Wang *et al.*, 2011). GRF9 (Wang *et al.*, 2011) as well as other miR396-regulated GRFs (Mecchia *et al.*, 2013) have been implicated in the control of cell proliferation that could also end in leaf polarity defects.

We found that at least *rGRF3* and 35S*:GRF5* can cause a delay in leaf senescence, while their loss-of-function mutations reduces the leaf longevity suggesting that a similar degree of redundancy can exist in the control of leaf size and senescence. Still, *rGRF3* can generate bigger leaves than *rGRF2* (this work) (Rodriguez *et al.*, 2010), so that quantitative differences in the activity of the GRFs might be expected *in vivo.* That we mainly detected GRF3 and GRF5 in the pull downs of GIF1-GFP is in agreement with this possibility and that GIF1 has a preferential association with certain GRFs *in vivo.* Interestingly, differences in the affinity between GRFs and GIFs have also been detected in yeast two-hybrid experiments (Liang *et al.*, 2013).

The GRFs seems to be deeply regulated post-transcriptionally at least at two different levels, by miR396 and by GIF co-regulators. Seven out of the nine Arabidopsis *GRFs* harbor a miR396 binding site (Jones-Rhoades and Bartel, 2004). In young developing leaves, miR396 controls the spatial expression of the *GRFs* restricting their activity to the proximal part of the organ, which in turn coincides with the cells undergoing mitosis (Rodriguez *et al.*, 2010; Debernardi *et al.*, 2012). At later stages of leaf development, miR396 repress the *GRFs* throughout the leaf (Rodriguez *et al.*, 2010). On the other hand, GIF1, whose domain of expression does not completely overlap with the GRFs can move from cell to cell (Kawade *et al.*, 2013). Therefore, the final GRF activity will integrate different cues like the levels of miRNA miR396 and GIF co-activators that might even be produced by neighboring cells. We hypothesize that GRF activity is under a strict quantitative regulation, which is important for fine-tuning the number of cells and longevity of the leaves (Figure 7).

EXPERIMENTAL PROCEDURES

Plant material and leaf analysis

Arabidopsis ecotype Col-0 and S96 were used in the experiments. Plants were grown either on soil or on Murashige and Skoog (MS) medium (Sigma, http://www.sigmaaldrich.com) in long (16 h light/8 h dark) or short photoperiods (8 h light/16 h dark) at 23°C. Leaf areas were measured using the ImageJ program (http://rsb.info.nih.gov/ij/) after dissection of individual leaves. The mutant alleles *grf5–1* (Salk086597), *grf3–1* (Salk026786), and *an3*-1 (CS241) were obtained from the Arabidopsis stock center. The *an3-4* mutants and 35S*:GRF5* plants were kindly provided by Prof. Dr Hirokazu Tsukaya and Prof. Dr Gorou Horiguchi (Horiguchi *et al.*, 2005).

Microscopic techniques

Confocal microscopy was performed on a Leica SPE DM5500 upright microscope using a ACS APO ×40/1.15 oil lens and using the LAS AF 1.8.2 software (http://www.leica.com). Green fluorescent protein (GFP) was excited with the 488-nm solid-state laser. The GFP emission was detected at a bandwidth of 505–530 nm, whereas the 'red' autofluorescence of chloroplasts was detected at a bandwidth of 600–800 nm.

To obtain paradermal views of palisade cells, leaves were fixed with formalin-acetic acid-alcohol and cleared with chloral hydrate solution (200 g chloral hydrate, 20 g glycerol, and 50 ml dH_2O) as described (Horiguchi *et al.*, 2005). Palisade leaf cells were observed using differential interference contrast microscopy. The density of palisade cells per unit area was determined, and the area of the leaf blade was divided by this value to calculate the total number of palisade cells in the subepidermal layer. To deter-

mine the cell area, 20 palisade cells were measured in each leaf. Experiments were carried out in duplicate with 10 leaves, obtaining similar results.

Transgenes

See Table S3 for a list of binary plasmids used in this study. The miRNA target motif in *GRF3* was altered introducing synonymous mutations in a cloned wild-type genomic fragment using the QuikChange Site Directed Mutagenesis Kit (Stratagene, La Jolla, CA, USA). Using Multisite Gateway cloning (Invitrogen™, http://www.lifetechnologies.com), an overexpression construct of *GIF1* under the control of the *Agrobacterium rhizogenes RolD* promoter and flanked with the *OCTOPINE SYNTHASE* (*OCS*) terminator was introduced into pKm43GW (Karimi *et al.*, 2007). The ANT:*GUS* and AS1:*GUS* vectors were kindly provided by Jia-Wei Wang and Detlef Weigel (Wang *et al.*, 2008). To generate ANT:*rGRF3* and AS1:*rGRF3* vectors, the *GUS* coding sequence was replaced by the *rGRF3* sequence. The 35S:*miR396b* line has been described previously (Mecchia *et al.*, 2013).

Expression analysis

RNA was extracted using TRIzol reagent (Invitrogen) and 1.0 mg of total RNA was treated with RQ1 RNase-free DNase (Promega, http://www.promega.com). Next, first-strand cDNA synthesis was carried out using SuperScript™ III Reverse Transcriptase (Invitrogen) with the appropriate primers. PCR reactions were performed in a Mastercycler® ep realplex thermal cycler (Eppendorf, http://www.eppendorf.com) using SYBRGreen I (Roche, http://www.roche.com) to monitor dsDNA synthesis. Relative transcript level was determined for each sample, normalized using *PROTEIN PHOSPHATASE 2A* (*AT1G13320*) cDNA levels. Primer sequences are given in Table S4. To visualize reporter activity, transgenic plants were subjected to GUS staining, as described previously (Donnelly *et al.*, 1999).

Statistical analysis

Data presented were analyzed using one-way analysis of variance (ANOVA), and to isolate the group or groups that differ from the others we used the Tukey's multiple comparison test. If needed, a rank-based ANOVA followed by Dunn's test was used. When comparing two data sets, Student's *t*-tests were used ($P < 0.05$), and significant differences were indicated with asterisks. In box plots, central lines indicated median values, boxes bound the 25th to 75th percentiles, and the whiskers indicated the 10th and 90th percentiles.

Microarray analysis

Total RNA was extracted from dissected vegetative apices of plants grown on short day photoperiod conditions for 20 days using the RNeasy plant mini kit (QIAGEN, http://www.qiagen.com). Microarray analyses using the Affymetrix ATH1 platform were performed on two biological replicates as described (Schommer *et al.*, 2008). Expression data were processed with Robin software (Lohse *et al.*, 2010) with the following settings, using the statistical analysis strategy: Limma, normalization method: gcrma, *P*-value cut-off value: 0.05. The expression levels of the differentially expressed genes across genotypes were normalized to the maximum expression value and then were K-means clustered with MultiExperiment Viewer (MEV) software, with a minimum limit of 5% of total genes per cluster. Functional enrichments were calculated with Chipenrich (Brady *et al.*, 2007). Microarrays files were deposited in the Gene Expression Omnibus database (GSE53458). Lists of genes affected by plant hormones were obtained from previously published data (Nemhauser *et al.*, 2006).

Dark-induced leaf senescence

Fully expanded fifth leaves were detached and floated on 3 mM MES (2-(N-Morpholino)-Ethanesulfonic acid, Genbiotech, Buenos Aires, Argentina) buffer solution (pH 5.7) and incubated at 23°C in darkness. As the leaves of *rGRF3* are larger than that of the wild-type, we collected fully expanded leaves immediately after they had finished their growth, so that the developmental time was adjusted independent of their sizes. To do this the sizes of the leaves were measured every day. The photochemical efficiency of PSII was deduced from the characteristics of chlorophyll fluorescence (Oh *et al.*, 1997). Variable fluorescence intensity/maximum fluorescence intensity (Fv/Fm) corresponds to the photochemical efficiency of PSII (Oh *et al.*, 1997).

Protein immunoprecipitation and MS

Protein immunoprecipitation (IP) experiments were essentially performed as described before (Smaczniak *et al.*, 2012b). During the IP, ethidium bromide was used to release protein complexes from the DNA and benzonase to degrade all forms of DNA and RNA and increase the specificity of the complex isolation. Plants without the transgene were used as a control.

ACKNOWLEDGEMENTS

We thank Jia-Wei Wang and Detlef Weigel for the vectors containing the *AS1* and *ANT* promoter, and Martin Sabatini for help in the construction of the reporters. JMD and MM were supported by fellowships from CONICET, JMD was also supported by an EMBO short term fellowship and Josefina Prats. RER and JP are members of CONICET. The majority of studies were supported by grants to JFP (ANPCyT). KK was supported by an Netherlands Organisation for Scientific Research VIDI grant. CS was supported by a grant from the Netherlands Proteomics Centre and Centre for BioSystems Genomics. DI and LV are supported by Ghent University ('Bijzonder Onderzoeksfonds Methusalem' Project BOF08/01M00408 and Multidisciplinary Research Partnership 'Biotechnology for a Sustainable Economy' Project 01MRB510W), the Belgian Science Policy Office (BELSPO) (IUAP VI/33), and the European Union FP6 ('AGRON-OMICS' Grant LSHG-CT-2006-037704).

SUPPORTING INFORMATION

Additional Supporting Information may be found in the online version of this article.

Figure S1. *GRF3* and *GIF1* transcript levels.

Figure S2. Genetic interaction between *GIF1* and *GRF5.*

Figure S3. Functions of *GRF3* in the absence of *GIF1.*

Figure S4. Genes repressed by overexpression of GRF3 and/or GIF1.

Figure S5. Leaf senescence of 35S:*GRF5* plants and *grf3* and *grf5* mutants.

Figure S6. Response of hormone regulated genes in 35S:*GIF1, rGRF3* and *rGRF3x*35S:*GIF1* microarrays.

Figure S7. Misexpression of *GRF3.*

Table S1 List of potential interaction partners enriched in the GIF1-GFP IP experiments.

Table S2 Analysis of genes changing in 35S:*GIF1, rGRF3* and *rGRF3x*35S:*GIF1* microarrays for enrichment of Gene Ontology.

Table S3 Binary plasmids used in this study.

Table S4 Relevant locus identifiers, mutant alleles and RT-qPCR primers.

Data S1. Transcriptome analysis of 35S:*GIF1, rGRF3* and *rGRF3x*35S:*GIF1* plants.

REFERENCES

Andriankaja, M., Dhondt, S., De Bodt, S. *et al.* (2012) Exit from proliferation during leaf development in *Arabidopsis thaliana*: a not-so-gradual process. *Dev. Cell*, **22**, 64–78.

Archacki, R., Sarnowski, T.J., Halibart-Puzio, J., Brzeska, K., Buszewicz, D., Prymakowska-Bosak, M., Koncz, C. and Jerzmanowski, A. (2009) Genetic analysis of functional redundancy of BRM ATPase and ATSWI3C subunits of Arabidopsis SWI/SNF chromatin remodelling complexes. *Planta*, **229**, 1281–1292.

Beemster, G.T., De Veylder, L., Vercruysse, S., West, G., Rombaut, D., Van Hummelen, P., Galichet, A., Gruissem, W., Inze, D. and Vuylsteke, M. (2005) Genome-wide analysis of gene expression profiles associated with cell cycle transitions in growing organs of Arabidopsis. *Plant Physiol.* **138**, 734–743.

Bezhani, S., Winter, C., Hershman, S., Wagner, J.D., Kennedy, J.F., Kwon, C.S., Pfluger, J., Su, Y. and Wagner, D. (2007) Unique, shared, and redundant roles for the Arabidopsis SWI/SNF chromatin-remodeling ATPases BRAHMA and SPLAYED. *Plant Cell*, **19**, 403–416.

Brady, S.M., Orlando, D.A., Lee, J.Y., Wang, J.Y., Koch, J., Dinneny, J.R., Mace, D., Ohler, U. and Benfey, P.N. (2007) A high-resolution root spatiotemporal map reveals dominant expression patterns. *Science*, **318**, 801–806.

Breeze, E., Harrison, E., McHattie, S. *et al.* (2011) High-resolution temporal profiling of transcripts during Arabidopsis leaf senescence reveals a distinct chronology of processes and regulation. *Plant Cell*, **23**, 873–894.

Chitwood, D.H., Guo, M., Nogueira, F.T. and Timmermans, M.C. (2007) Establishing leaf polarity: the role of small RNAs and positional signals in the shoot apex. *Development*, **134**, 813–823.

Cosgrove, D.J. (2005) Growth of the plant cell wall. *Nat. Rev. Mol. Cell Biol.* **6**, 850–861.

Debernardi, J.M., Rodriguez, R.E., Mecchia, M.A. and Palatnik, J.F. (2012) Functional specialization of the plant miR396 fulfillwork through distinct microRNA-target interactions. *PLoS Genet.* **8**, e1002419.

Donnelly, P.M., Bonetta, D., Tsukaya, H., Dengler, R.E. and Dengler, N.G. (1999) Cell cycling and cell enlargement in developing leaves of Arabidopsis. *Dev. Biol.* **215**, 407–419.

Efroni, I., Han, S.K., Kim, H.J., Wu, M.F., Steiner, E., Birnbaum, K.D., Hong, J.C., Eshed, Y. and Wagner, D. (2013) Regulation of leaf maturation by chromatin-mediated modulation of cytokinin responses. *Dev. Cell*, **24**, 438–445.

Ellis, C.M., Nagpal, P., Young, J.C., Hagen, G., Guilfoyle, T.J. and Reed, J.W. (2005) AUXIN RESPONSE FACTOR1 and AUXIN RESPONSE FACTOR2 regulate senescence and floral organ abscission in *Arabidopsis thaliana*. *Development*, **132**, 4563–4574.

Farrona, S., Hurtado, L., Bowman, J.L. and Reyes, J.C. (2004) The *Arabidopsis thaliana* SNF2 homolog AtBRM controls shoot development and flowering. *Development*, **131**, 4965–4975.

Gonzalez, N., De Bodt, S., Sulpice, R. *et al.* (2010) Increased leaf size: different means to an end. *Plant Physiol.* **153**, 1261–1279.

Gonzalez, N., Vanhaeren, H. and Inze, D. (2012) Leaf size control: complex co-ordination of cell division and expansion. *Trends Plant Sci.* **17**, 332–340.

Haga, N., Kato, K., Murase, M. *et al.* (2007) R1R2R3-Myb proteins positively regulate cytokinesis through activation of KNOLLE transcription in *Arabidopsis thaliana*. *Development*, **134**, 1101–1110.

Horiguchi, G. and Tsukaya, H. (2011) Organ size regulation in plants: insights from compensation. *Front. Plant Sci.* **2**, 24.

Horiguchi, G., Kim, G.T. and Tsukaya, H. (2005) The transcription factor AtGRF5 and the transcription coactivator AN3 regulate cell proliferation in leaf primordia of *Arabidopsis thaliana*. *Plant J.* **43**, 68–78.

Horiguchi, G., Nakayama, H., Ishikawa, N., Kubo, M., Demura, T., Fukuda, H. and Tsukaya, H. (2011) ANGUSTIFOLIA3 plays roles in adaxial/abaxial patterning and growth in leaf morphogenesis. *Plant Cell Physiol.* **52**, 112–124.

Hurtado, L., Farrona, S. and Reyes, J.C. (2006) The putative SWI/SNF complex subunit BRAHMA activates flower homeotic genes in *Arabidopsis thaliana*. *Plant Mol. Biol.* **62**, 291–304.

Jerzmanowski, A. (2007) SWI/SNF chromatin remodeling and linker histones in plants. *Biochim. Biophys. Acta*, **1769**, 330–345.

Jones-Rhoades, M.W. and Bartel, D.P. (2004) Computational identification of plant microRNAs and their targets, including a stress-induced miRNA. *Mol. Cell*, **14**, 787–799.

Karimi, M., Depicker, A. and Hilson, P. (2007) Recombinational cloning with plant gateway vectors. *Plant Physiol.* **145**, 1144–1154.

Kawade, K., Horiguchi, G. and Tsukaya, H. (2010) Non-cell-autonomously coordinated organ size regulation in leaf development. *Development*, **137**, 4221–4227.

Kawade, K., Horiguchi, G., Usami, T., Hirai, M.Y. and Tsukaya, H. (2013) ANGUSTIFOLIA3 signaling coordinates proliferation between clonally distinct cells in leaves. *Curr. Biol.* **23**, 788–792.

Kidner, C.A. and Martienssen, R.A. (2004) Spatially restricted microRNA directs leaf polarity through ARGONAUTE1. *Nature*, **428**, 81–84.

Kim, J.H. and Kende, H. (2004) A transcriptional coactivator, AtGIF1, is involved in regulating leaf growth and morphology in Arabidopsis. *Proc. Natl Acad. Sci. USA*, **101**, 13374–13379.

Kim, J.H. and Lee, B.H. (2006) GROWTH-REGULATING FACTOR4 of *Arabidopsis thaliana* is required for development of leaves, cotyledons, and shoot apical meristem. *J. Plant Biol.* **49**, 463–468.

Kim, J.H., Choi, D. and Kende, H. (2003) The AtGRF family of putative transcription factors is involved in leaf and cotyledon growth in Arabidopsis. *Plant J.* **36**, 94–104.

Kim, J.H., Woo, H.R., Kim, J., Lim, P.O., Lee, I.C., Choi, S.H., Hwang, D. and Nam, H.G. (2009) Trifurcate feed-forward regulation of age-dependent cell death involving miR164 in Arabidopsis. *Science*, **323**, 1053–1057.

Kim, J.S., Mizoi, J., Kidokoro, S. *et al.* (2012) Arabidopsis growth-regulating factor7 functions as a transcriptional repressor of abscisic acid- and osmotic stress-responsive genes, including DREB2A. *Plant Cell*, **24**, 3393–3405.

Kozuka, T., Horiguchi, G., Kim, G.T., Ohgishi, M., Sakai, T. and Tsukaya, H. (2005) The different growth responses of the *Arabidopsis thaliana* leaf blade and the petiole during shade avoidance are regulated by photoreceptors and sugar. *Plant Cell Physiol.* **46**, 213–223.

Kuijt, S.J., Greco, R., Agalou, A. *et al.* (2014) Interaction between the GRF and KNOX families of transcription factors. *Plant Physiol.* **164**, 1952–1966.

Kwon, C.S. and Wagner, D. (2007) Unwinding chromatin for development and growth: a few genes at a time. *Trends Genet.* **23**, 403–412.

Kwon, C.S., Hibara, K., Pfluger, J., Bezhani, S., Metha, H., Aida, M., Tasaka, M. and Wagner, D. (2006) A role for chromatin remodeling in regulation of CUC gene expression in the Arabidopsis cotyledon boundary. *Development*, **133**, 3223–3230.

Lee, B.H., Ko, J.H., Lee, S., Lee, Y., Pak, J.H. and Kim, J.H. (2009) The Arabidopsis GRF-INTERACTING FACTOR gene family performs an overlapping function in determining organ size as well as multiple developmental properties. *Plant Physiol.* **151**, 655–668.

Liang, G., He, H., Li, Y., Wang, F. and Yu, D. (2013) Molecular mechanism of miR396 mediating pistil development in *Arabidopsis thaliana*. *Plant Physiol.* **164**, 249–258.

Lim, P.O., Kim, H.J. and Nam, H.G. (2007) Leaf senescence. *Annu. Rev. Plant Biol.* **58**, 115–136.

Lim, P.O., Lee, I.C., Kim, J., Kim, H.J., Ryu, J.S., Woo, H.R. and Nam, H.G. (2010) Auxin response factor 2 (ARF2) plays a major role in regulating auxin-mediated leaf longevity. *J. Exp. Bot.* **61**, 1419–1430.

Liu, D., Song, Y., Chen, Z. and Yu, D. (2009) Ectopic expression of miR396 suppresses GRF target gene expression and alters leaf growth in Arabidopsis. *Physiol. Plant.* **136**, 223–236.

Lohse, M., Nunes-Nesi, A., Kruger, P. *et al.* (2010) Robin: an intuitive wizard application for R-based expression microarray quality assessment and analysis. *Plant Physiol.* **153**, 642–651.

Mecchia, M.A., Debernardi, J.M., Rodriguez, R.E., Schommer, C. and Palatnik, J.F. (2013) MicroRNA miR396 and RDR6 synergistically regulate leaf development. *Mech. Dev.* **130**, 2–13.

Nagai, M., Tanaka, S., Tsuda, M. *et al.* (2001) Analysis of transforming activity of human synovial sarcoma-associated chimeric protein SYT-SSX1

bound to chromatin remodeling factor hBRM/hSNF2 alpha. *Proc. Natl Acad. Sci. USA*, **98**, 3843–3848.

Nemhauser, J.L., Hong, F. and Chory, J. (2006) Different plant hormones regulate similar processes through largely nonoverlapping transcriptional responses. *Cell*, **126**, 467–475.

Noh, Y.S. and Amasino, R.M. (1999) Identification of a promoter region responsible for the senescence-specific expression of SAG12. *Plant Mol. Biol.* **41**, 181–194.

Oh, S.A., Lee, S.Y., Chung, I.K., Lee, C.H. and Nam, H.G. (1996) A senescence-associated gene of *Arabidopsis thaliana* is distinctively regulated during natural and artificially induced leaf senescence. *Plant Mol. Biol.* **30**, 739–754.

Oh, S.A., Park, J.H., Lee, G.I., Paek, K.H., Park, S.K. and Nam, H.G. (1997) Identification of three genetic loci controlling leaf senescence in *Arabidopsis thaliana*. *Plant J.* **12**, 527–535.

Okushima, Y., Mitina, I., Quach, H.L. and Theologis, A. (2005) AUXIN RESPONSE FACTOR 2 (ARF2): a pleiotropic developmental regulator. *Plant J.* **43**, 29–46.

Park, J.H., Oh, S.A., Kim, Y.H., Woo, H.R. and Nam, H.G. (1998) Differential expression of senescence-associated mRNAs during leaf senescence induced by different senescence-inducing factors in Arabidopsis. *Plant Mol. Biol.* **37**, 445–454.

Perani, M., Ingram, C.J., Cooper, C.S., Garrett, M.D. and Goodwin, G.H. (2003) Conserved SNH domain of the proto-oncoprotein SYT interacts with components of the human chromatin remodelling complexes, while the QPGY repeat domain forms homo-oligomers. *Oncogene*, **22**, 8156–8167.

Pulido, A. and Laufs, P. (2010) Co-ordination of developmental processes by small RNAs during leaf development. *J. Exp. Bot.* **61**, 1277–1291.

Rodriguez, R.E., Mecchia, M.A., Debernardi, J.M., Schommer, C., Weigel, D. and Palatnik, J.F. (2010) Control of cell proliferation in *Arabidopsis thaliana* by microRNA miR396. *Development*, **137**, 103–112.

Rubio-Somoza, I. and Weigel, D. (2011) MicroRNA networks and developmental plasticity in plants. *Trends Plant Sci.* **16**, 258–264.

Sarnowski, T.J., Rios, G., Jasik, J. *et al.* (2005) SWI3 subunits of putative SWI/SNF chromatin-remodeling complexes play distinct roles during Arabidopsis development. *Plant Cell*, **17**, 2454–2472.

Schmid, M., Davison, T.S., Henz, S.R., Pape, U.J., Demar, M., Vingron, M., Scholkopf, B., Weigel, D. and Lohmann, J.U. (2005) A gene expression map of *Arabidopsis thaliana* development. *Nat. Genet.* **37**, 501–506.

Schommer, C., Palatnik, J.F., Aggarwal, P., Chetelat, A., Cubas, P., Farmer, E.E., Nath, U. and Weigel, D. (2008) Control of jasmonate biosynthesis and senescence by miR319 targets. *PLoS Biol.* **6**, e230.

Schruff, M.C., Spielman, M., Tiwari, S., Adams, S., Fenby, N. and Scott, R.J. (2006) The AUXIN RESPONSE FACTOR 2 gene of Arabidopsis links auxin signalling, cell division, and the size of seeds and other organs. *Development*, **133**, 251–261.

Smaczniak, C., Immink, R.G., Muino, J.M. *et al.* (2012a) Characterization of MADS-domain transcription factor complexes in Arabidopsis flower development. *Proc. Natl Acad. Sci. USA*, **109**, 1560–1565.

Smaczniak, C., Li, N., Boeren, S., America, T., van Dongen, W., Goerdayal, S.S., de Vries, S., Angenent, G.C. and Kaufmann, K. (2012b) Proteomics-based identification of low-abundance signaling and regulatory protein complexes in native plant tissues. *Nat. Protoc.* **7**, 2144–2158.

Thaete, C., Brett, D., Monaghan, P., Whitehouse, S., Rennie, G., Rayner, E., Cooper, C.S. and Goodwin, G. (1999) Functional domains of the SYT and SYT-SSX synovial sarcoma translocation proteins and co-localization with the SNF protein BRM in the nucleus. *Hum. Mol. Genet.* **8**, 585–591.

Tsukaya, H. (2005) Leaf shape: genetic controls and environmental factors. *Int. J. Dev. Biol.* **49**, 547–555.

Van Leene, J., Stals, H., Eeckhout, D. *et al.* (2007) A tandem affinity purification-based technology platform to study the cell cycle interactome in *Arabidopsis thaliana*. *Mol. Cell. Proteomics* **6**, 1226–1238.

Van Leene, J., Witters, E., Inze, D. and De Jaeger, G. (2008) Boosting tandem affinity purification of plant protein complexes. *Trends Plant Sci.* **13**, 517–520.

Vercruyssen, L., Verkest, A., Gonzalez, N. *et al.* (2014) ANGUSTIFOLIA3 Binds to SWI/SNF Chromatin remodeling complexes to regulate transcription during Arabidopsis leaf development. *Plant Cell*, **26**, 210–229.

Wagner, D. and Meyerowitz, E.M. (2002) SPLAYED, a novel SWI/SNF ATPase homolog, controls reproductive development in Arabidopsis. *Curr. Biol.* **12**, 85–94.

Wang, J.W., Schwab, R., Czech, B., Mica, E. and Weigel, D. (2008) Dual effects of miR156-targeted SPL genes and CYP78A5/KLUH on plastochron length and organ size in *Arabidopsis thaliana*. *Plant Cell*, **20**, 1231–1243.

Wang, J.W., Czech, B. and Weigel, D. (2009) miR156-regulated SPL transcription factors define an endogenous flowering pathway in *Arabidopsis thaliana*. *Cell*, **138**, 738–749.

Wang, L., Gu, X., Xu, D., Wang, W., Wang, H., Zeng, M., Chang, Z., Huang, H. and Cui, X. (2011) miR396-targeted AtGRF transcription factors are required for co-ordination of cell division and differentiation during leaf development in Arabidopsis. *J. Exp. Bot.* **62**, 761–773.

Wu, G. and Poethig, R.S. (2006) Temporal regulation of shoot development in *Arabidopsis thaliana* by miR156 and its target SPL3. *Development*, **133**, 3539–3547.

Wu, G., Park, M.Y., Conway, S.R., Wang, J.W., Weigel, D. and Poethig, R.S. (2009) The sequential action of miR156 and miR172 regulates developmental timing in Arabidopsis. *Cell*, **138**, 750–759.

Wu, M.F., Sang, Y., Bezhani, S., Yamaguchi, N., Han, S.K., Li, Z., Su, Y., Slewinski, T.L. and Wagner, D. (2012) SWI2/SNF2 chromatin remodeling ATPases overcome polycomb repression and control floral organ identity with the LEAFY and SEPALLATA3 transcription factors. *Proc. Natl Acad. Sci. USA*, **109**, 3576–3581.